nature nanotechnology

Article

https://doi.org/10.1038/s41565-022-01278-y

Highly stable, antiviral, antibacterial cotton textiles via molecular engineering

Received: 4 April 2022

Accepted: 27 October 2022

Published online: 30 December 2022

Check for updates

Ji Qian[1,11], Qi Dong[1,11], Kayla Chun[2,3,4,11], Dongyang Zhu[1,11], Xin Zhang[1], Yimin Mao[1,5], James N. Culver[3,6], Sheldon Tai[7], Jennifer R. German[7], David P. Dean[8], Jeffrey T. Miller[8], Liguang Wang[9], Tianpin Wu[9], Tian Li[1], Alexandra H. Brozena[1], Robert M. Briber[1], Donald K. Milton[6], William E. Bentley[2,3,4] ✉ & Liangbing Hu[1,10] ✉

Cotton textiles are ubiquitous in daily life and are also one of the primary mediums for transmitting viruses and bacteria. Conventional approaches to fabricating antiviral and antibacterial textiles generally load functional additives onto the surface of the fabric and/or their microfibres. However, such modifications are susceptible to deterioration after long-term use due to leaching of the additives. Here we show a different method to impregnate copper ions into the cellulose matrix to form a copper ion-textile (Cu-IT), in which the copper ions strongly coordinate with the oxygen-containing polar functional groups (for example, hydroxyl) of the cellulose chains. The Cu-IT displays high antiviral and antibacterial performance against tobacco mosaic virus and influenza A virus, and *Escherichia coli*, *Salmonella typhimurium*, *Pseudomonas aeruginosa* and *Bacillus subtilis* bacteria due to the antimicrobial properties of copper. Furthermore, the strong coordination bonding of copper ions with the hydroxyl functionalities endows the Cu-IT with excellent air/water retainability and superior mechanical stability, which can meet daily use and resist repeated washing. This method to fabricate Cu-IT is cost-effective, ecofriendly and highly scalable, and this textile appears very promising for use in household products, public facilities and medical settings.

Frequent outbreaks of epidemics in recent years, including influenza, gastroenteritis, tuberculosis, pneumonia and particularly the coronavirus disease 2019 (COVID-19), have claimed numerous human lives worldwide[1–3]. These diseases can spread through human activities, where clothing and other textiles are primary vectors for the culture and transfer of viral and bacterial species[4–8]. In recent decades, researchers have investigated various approaches to incorporating antiviral and antibacterial properties into cotton textiles due to their universal use. Cotton textiles are composed of hierarchical microstructures that consist of cellulose molecules, which are polymers derived from D-glucose

[1]Department of Materials Science and Engineering, University of Maryland, College Park, MD, USA. [2]Fischell Department of Bioengineering, University of Maryland, College Park, MD, USA. [3]Institute for Bioscience and Biotechnology Research, University of Maryland, College Park, MD, USA. [4]Robert E. Fischell Institute for Biomedical Devices, University of Maryland, College Park, MD, USA. [5]NIST Center for Neutron Research, National Institute of Standards and Technology (NIST), Gaithersburg, MD, USA. [6]Department of Plant Science and Landscape Architecture, University of Maryland, College Park, MD, USA. [7]Maryland Institute for Applied Environmental Health, University of Maryland, College Park, MD, USA. [8]Davidson School of Chemical Engineering, Purdue University, West Lafayette, IN, USA. [9]X-ray Science Division, Argonne National Laboratory, Lemont, IL, USA. [10]Center for Materials Innovation, University of Maryland, College Park, MD, USA. [11]These authors contributed equally: Ji Qian, Qi Dong, Kayla Chun, Dongyang Zhu. ✉e-mail: bentley@umd.edu; binghu@umd.edu

https://doi.org/10.1038/s41565-022-01278-y

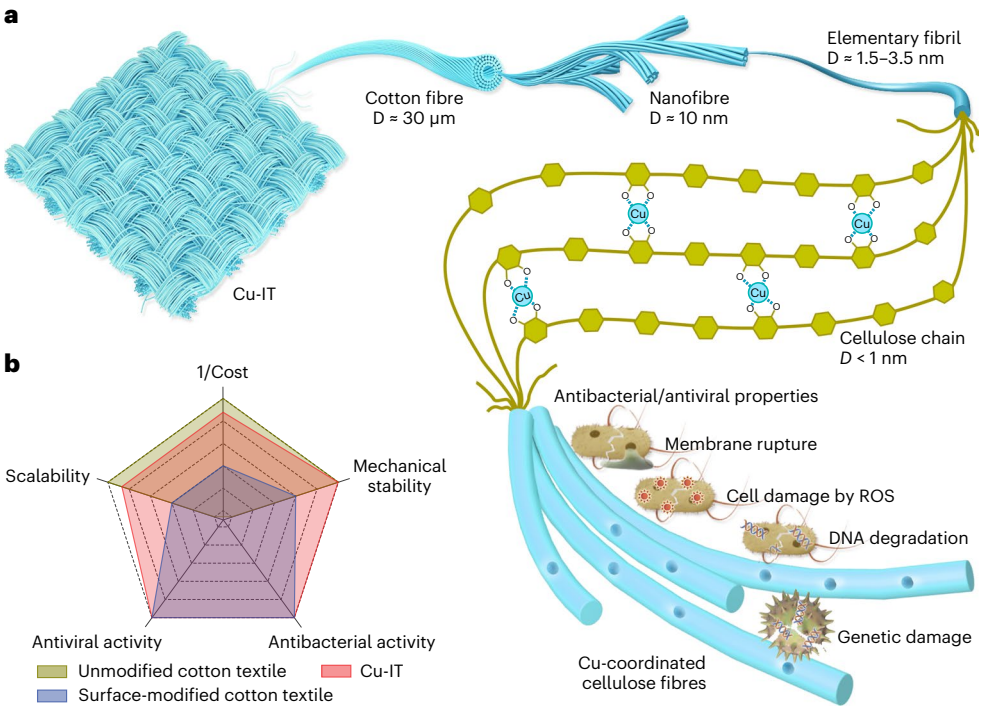

Fig. 1 | The structure and performance of the Cu-IT. a, Schematic showing the structure of the Cu-IT and the proposed mechanism of its antiviral and antibacterial properties. The coordinated copper ions within the cellulose fibres can interact with the viral genome and prevent the virus from replicating. Additionally, the copper ions cause bacterial cell membrane rupture, resulting in a loss of the membrane potential and cytoplasmic content; they can also induce the production of ROS, leading to denaturation of DNA and cell death. **b**, A comparison of the performance of the Cu-IT to that of unmodified and surface-modified cotton textiles (Supplementary Note 1).

monomers via the linkage of β-(1,4) glycosidic bonds[9,10]. Cellulose polymers are typically biosynthesized from cellulose synthase complex (CSC)[11,12] and form as elementary fibrils of approximately 1.5–3.5 nm in diameter. These elementary fibrils can further self-assemble into larger bundles, termed cellulose nanofibres, with a nominal cross-sectional size of ~10 nm, which ultimately form microfibres with diameters of decadal micrometres. However, current mainstream strategies for producing antiviral and antibacterial textiles only physically load antiviral and antibacterial additives onto the fabric and do not fully leverage the material's molecular structures. For example, a range of antiviral and antimicrobial agents, such as organic compounds (for example, quaternary ammonium compounds, triclosan, polyhexamethylene biguanide and *N*-halamines), synthetic or natural polymers (for example, polypyrrole, chitosan and specific natural dyes), graphene materials and metal-based materials (for example, copper, silver and zinc, and their oxides and salts), have been physically incorporated into textiles[13–17]. In a specific example, cotton textiles coated with metallic copper, Cu_2O and CuO nanoparticles were shown to exhibit high antiviral and antibacterial effects[18–22]. However, these additives are typically introduced into the textiles via methods such as vapour deposition, evaporation, sputtering and spraying, which raises concerns about the coating durability against wearing and washing due to low adhesivity, weak mechanical strength and limited bonding ability (for example, weak electrostatic interactions)[15]. In addition, the high expense and difficulty of scaling up prevent the wide application of these methods.

Here we introduce a new strategy of fabricating antimicrobial cotton textiles based on a fundamentally different principle of incorporating copper ions into the cotton structure at the molecular level, utilizing strong coordination bonding between copper ions and the cellulose molecules. This new approach can produce antiviral and antibacterial cotton textiles that are wearable and washable in a scalable and cost-effective manner, enabling practical application in everyday use. The method employs a strategy of disrupting the hydrogen-bonding network interconnecting the cellulose chains, followed by diffusing Cu(II) ions into the swollen cellulosic materials, allowing them to coordinate with the hydroxyl groups on the cellulose chains and form a stable copper ion–cellulose complex (Fig. 1a). The two processes are accomplished via a one-pot reaction by soaking a cotton textile in a Cu(II)-saturated NaOH solution. The coordination bonding between copper ions and their neighbouring cellulose chains makes this copper ion-textile (Cu-IT) highly stable in air and water, and durable against abrasion. The copper ions can interact with viral genomes and inhibit virus replication[23–25], and cause contact killing of bacteria and fungi by rupturing cell membranes and inducing reactive oxygen species (ROS)[26–29]. Cu-IT also shows better mechanical properties, with a ~23% increase in tensile strength compared with unmodified textiles, which is due to the role of the copper ions as 'crosslinkers' between the cellulose molecular chains. As a proof-of-concept, we show that Cu-IT exhibits high antiviral and antibacterial activities against tobacco mosaic virus (TMV), influenza A virus (IAV), and *Escherichia coli*, *Salmonella typhimurium*, *Pseudomonas aeruginosa* and *Bacillus subtilis* bacteria. Additionally, the fabrication of Cu-IT is simple, scalable and cost-effective, and can be applied to different types of cotton fabrics (Fig. 1b). This methodology may provide a renewed understanding of the potential of cellulosic materials, adding new dimensions to their application, including improved public health and hygiene.

Material synthesis and characterization

The Cu-IT fabrication process only requires a simple set-up and inexpensive chemicals. First, a piece of cotton textile was immersed in a blue Cu(II)-saturated aqueous NaOH solution until no further colour change was observed in the fabric. Then, the blue textile was taken out and washed with deionized (DI) water to remove residual NaOH and excess Cu(II) ions. Finally, the textile was dried, ready for further use (see Methods for more details). Visual inspection of the unmodified textile and Cu-IT (20 cm × 8 cm) is shown in Fig. 2a,b. The control parameters

https://doi.org/10.1038/s41565-022-01278-y

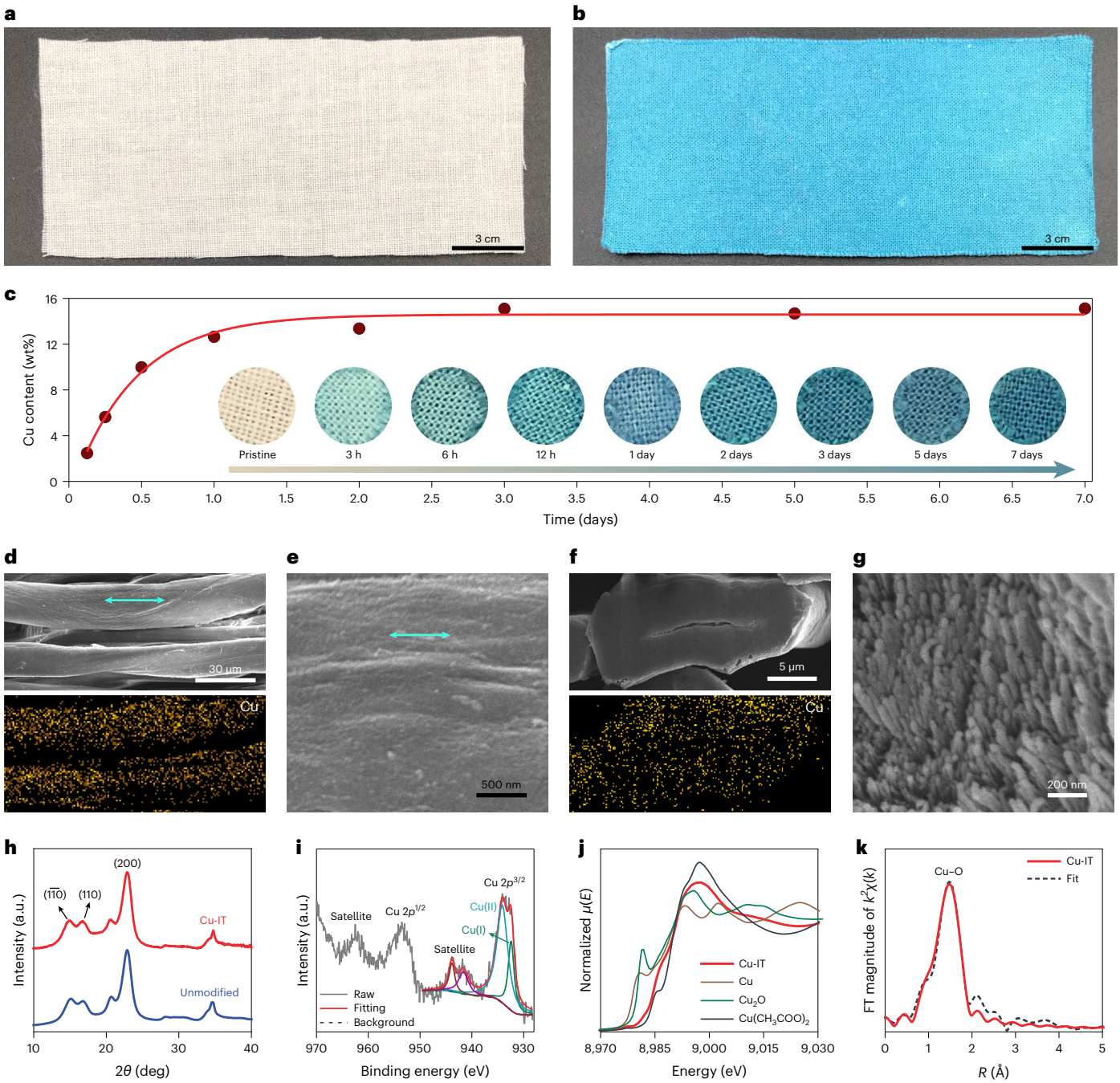

Fig. 2 | Characterization of the Cu-IT. a,**b**, Photographs of the unmodified cotton textile (**a**) and the Cu-IT (**b**) (20 cm × 8 cm). **c**, The copper contents in the Cu-IT samples produced using different soaking times. Insets: corresponding photographs of the textile samples. **d**, SEM micrograph of the cotton microfibres within the Cu-IT and the corresponding copper elemental mapping. **e**, Higher-magnification SEM micrograph of the Cu-IT. **f**, Cross-sectional SEM micrograph of a Cu-IT microfibre and the corresponding copper elemental mapping. **g**, Higher-magnification cross-sectional SEM micrograph of elementary fibrils that constitutes the microfibres of the Cu-IT. **h**, X-ray diffraction profile of the unmodified textile and Cu-IT. **i**, XPS Cu 2*p* spectrum of the Cu-IT. **j**, Cu K-edge XANES spectra of the Cu-IT; spectra of Cu, Cu_2O, and $Cu(CH_3COO)_2$ standards are shown for comparison purposes. **k**, *R*-space EXAFS spectrum of the Cu-IT and the corresponding fitting curve. FT, Fourier transform.

of the fabrication process include the NaOH concentration and soaking time. We first examined the influence of the NaOH concentration on the Cu(II) ion coordination (Supplementary Note 2). Supplementary Figs. 1 and 2 show photographs of the textiles immersed in Cu(II)-saturated NaOH solutions at four different NaOH concentrations (5, 10, 20 and 40 wt%), which confirmed that higher NaOH concentration does not always promote Cu(II) coordination. For example, textiles soaked in 5 and 10 wt% NaOH solutions completely changed colour and turned dark blue within 1 day, while the textile in 40 wt% NaOH solution only showed a much lighter and uneven blue colour during the same period. Next, the four samples were washed to a near-neutral condition with DI water and vacuum dried for thermogravimetric analysis (TGA) to determine the copper content (Supplementary Fig. 3 and Supplementary Note 3). The sample treated with 10 wt% NaOH solution featured the highest copper content (~8.43 wt%). Therefore, we used the 10 wt% NaOH solution to prepare all Cu-IT samples described hereafter. We also investigated the change in the copper content in the Cu-ITs fabricated under different soaking times (Fig. 2c and Supplementary Fig. 4). Initially, the copper

https://doi.org/10.1038/s41565-022-01278-y

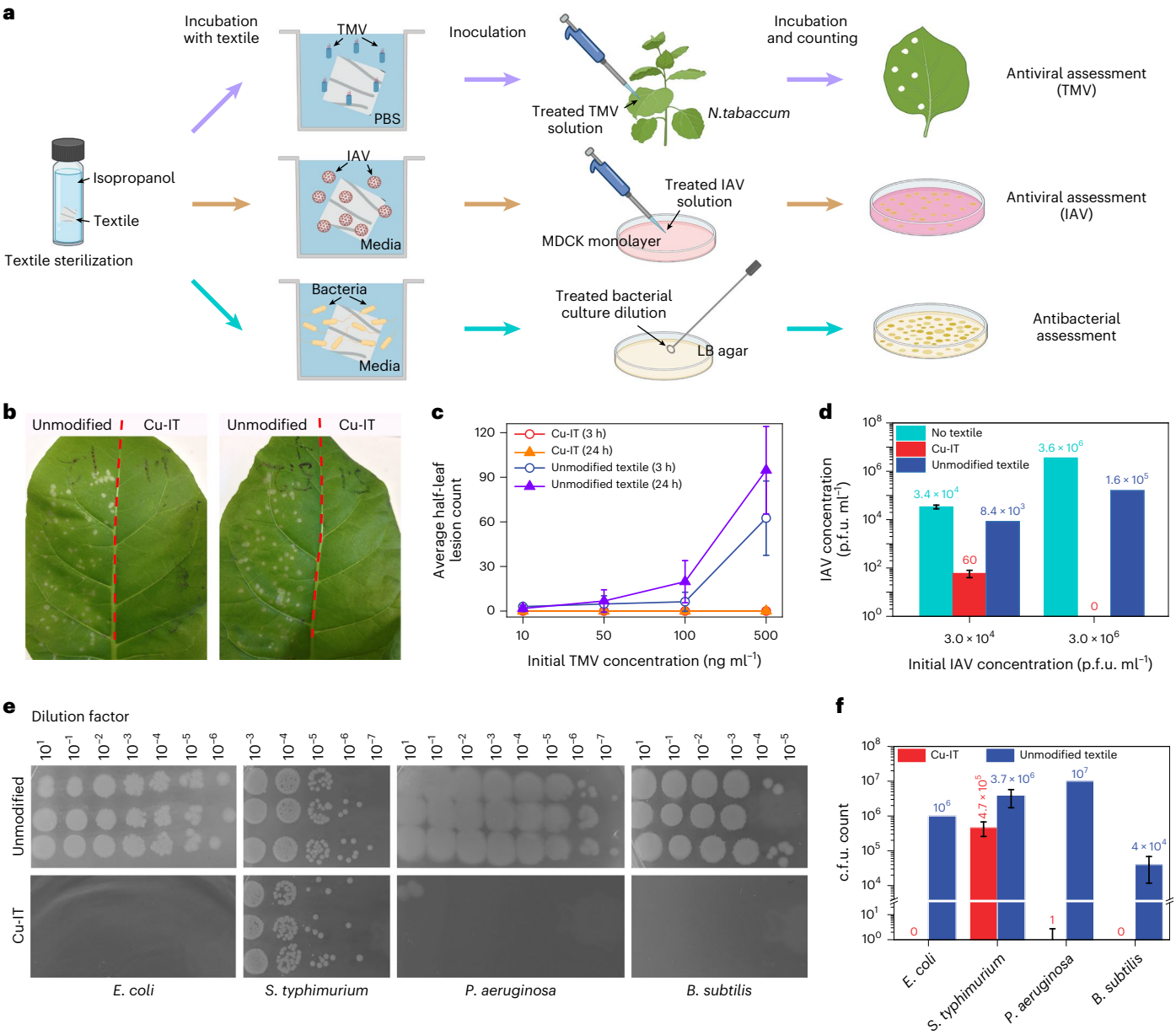

Fig. 3 | The antiviral and antibacterial activity of the Cu-IT. a, Schematic of the antiviral and antibacterial tests of the textiles. The unmodified and Cu-IT samples are first sterilized in isopropanol. For antiviral assessment, the sterilized textiles are incubated in TMV and IAV solutions. To assess infectivity of the textile-treated TMV, the treated TMV solution is applied to a tobacco leaf and the resulting virus-induced lesions are counted after growing the plant for 5 days. To assess the infectivity of the textile-treated IAV, the treated IAV solutions were inoculated on MDCK cells, and the plaques formed on the MDCK cell monolayer were counted after 3 days of incubation. For antibacterial assessment, the sterilized textiles were incubated in liquid bacterial cultures. The cultures were then measured for bacteria viability by plating them onto solid growth media and counting the resulting colonies. Created with BioRender.com. **b**, Photographs of the leaves tested with 500 ng ml^{-1} TMV from the infectivity assay at 3 h (left) and 24 h (right). The left and right halves of the leaves were inoculated with TMV solutions that had been treated by the unmodified textile and Cu-IT, respectively. **c**, Average half-leaf lesion counts ($n = 4$) of the two sides of the leaves that had been inoculated with different TMV solutions. The TMV solutions were pretreated with the unmodified textile (blue and purple) and Cu-IT (red and orange) and then treated for 3 h (open circle markers) and 24 h (solid triangle markers), respectively. The error bars represent the standard deviation of half-leaf lesion count. **d**, Infectivity of low (3×10^4 p.f.u. ml^{-1}) and high (3×10^6 p.f.u. ml^{-1}) concentration IAV after incubation without textile, with Cu-IT and with unmodified textile. The error bars represent the standard deviation of IAV concentration. **e**, Photographs of the LB agar plates after the inoculation and overnight incubation of the unmodified textile (top) and the Cu-IT (bottom) treated bacteria cultures, including *E. coli*, *S. typhimurium*, *P. aeruginosa* and *B. subtilis* bacteria. **f**, c.f.u. counts measured from the antibacterial assay shown in **e**. The error bars represent the standard deviation of c.f.u. count.

content increased with the reaction time and plateaued at 12.64 wt% after soaking for 1 day.

Scanning electron microscopy (SEM) micrographs reveal that the Cu(II)-saturated NaOH solution does not change the morphology of the textiles (Supplementary Fig. 5). Importantly, no particles are observed on the surfaces of the cellulose microfibres (Fig. 2d) and nanofibres (Fig. 2e) of the Cu-IT, indicating the absence of copper salts or oxides. We also used energy dispersive spectroscopy (EDS) to confirm the uniform distribution of copper throughout the cellulose microfibres (bottom of Fig. 2d and Supplementary Fig. 6). Additionally, no sodium is observed in the EDS spectrum in Supplementary Fig. 6, suggesting that NaOH has been thoroughly removed during the washing process.

Finally, the cross-sectional morphology and copper mapping of the microfibres revealed by SEM imaging and EDS analysis (Fig. 2f,g and Supplementary Fig. 7) confirm the well-preserved microstructures of the cotton fibres and the even distribution of the copper ions throughout the fibres. Our strategy of incorporating copper ions into the microfibres leads to a more homogeneous distribution of copper compared with prior antimicrobial cotton fabrics, in which copper particles were deposited on the fibre surfaces[18–22]. Therefore, we hypothesize that the copper ions of the Cu-IT should be more stable.

We further studied the copper insertion mechanism. Two processes occur with the textiles during soaking in the Cu(II)-saturated NaOH solution. The alkaline environment effectively disrupts the existing hydrogen-bonding networks[30,31], resulting in a swollen cellulose matrix. Next, the Cu(II) ions can diffuse into the cellulose crystals and the gaps between crystals to coordinate with oxygen atoms of the hydroxyl groups on the cellulose chains. Note that the crystal structure of cellulose also changes from cellulose-I[32] with parallel chain packing to cellulose-II with antiparallel packing[33] during the first process. Such molecular conformations and packing modes provide optimal geometries for copper coordination to form a new crystal structure of Na-cellulose II(Cu)[34,35], as verified by X-ray diffraction analysis (Supplementary Fig. 8). After removing NaOH by washing with DI water and drying, the expanded Na-cellulose II(Cu) lattices collapse and the cellulose-I lattices are recovered, which is shown by the resemblance between the X-ray diffraction patterns of the unmodified textile and Cu-IT (Fig. 2h); additionally, no signature diffraction peaks associated with new crystal structures are observed.

The copper ions, however, are trapped between the unit cells of cellulose crystals, which we confirmed by two major experimental observations. First, the results from X-ray photoelectron spectroscopy (XPS) indicate the presence of copper species in the Cu-IT. The Cu 2*p* XPS spectrum of the Cu-IT (Fig. 2i) shows a Cu $2p^{3/2}$ peak at 933.4 eV and an apparent satellite peak at 943 eV, indicating a mixed Cu(I) and Cu(II) state[36,37]. The appearance of a small amount of Cu(I) may be attributed to the weak reducing ability of cellulose[38,39]. We also note that a sodium signal is not detected (Supplementary Fig. 9), consistent with the EDS results of the Cu-IT (Supplementary Fig. 6), confirming that NaOH has been completely removed. Second, the coordinated state of copper ions in the Cu-IT textile was verified by X-ray absorption spectroscopy (XAS). The Cu K-edge X-ray absorption near-edge structure (XANES) spectrum of the Cu-IT (Fig. 2j) shows a broadened characteristic Cu(II) signature. A first-shell Cu–O bonding featuring a distance of 1.93 Å and a copper coordination number of 4.0 (Supplementary Tables 1 and 2) were determined by fitting the extended X-ray absorption fine structure (EXAFS) spectrum of the Cu-IT (Fig. 2k). These spectroscopic findings, along with the results from calorimetric experiments and macroscopic properties such as the stable colour, indicate that copper ions are trapped in the cellulose matrix and stabilized via coordination bonding.

Antiviral and antibacterial activity

We tested the antiviral and antibacterial properties of the Cu-IT (Fig. 3a). TMV and IAV were used as model viruses, and *E. coli, S. typhimurium, P. aeruginosa* and *B. subtilis* as model bacteria. The viral or bacterial strains were first incubated in the presence of the unmodified cotton textile control or Cu-IT (both textiles were sterilized before use). Then, the viruses and bacteria were inoculated on appropriate media to test the viral infectivity and bacterial viability. To assess the infectivity of TMV, one half of a *Nicotiana tabaccum* leaf was inoculated with the Cu-IT-treated TMV and the other half with the unmodified textile-treated control. The number of lesions on the leaf after 5 days of plant growth was counted as a measure of the TMV infectivity. Meanwhile, to assess the infectivity of IAV, the textile-treated IAV solutions were inoculated on Madin–Darby canine kidney (MDCK) cells, and plaques formed on the MDCK cell monolayer after 3 days of incubation were counted. For the antibacterial assessment, cell viability was measured by replicate plating of bacterial cultures (treated with the unmodified textile or Cu-IT) onto Luria–Bertani broth (LB) agar, and the agar plates were then counted for colonies after incubation overnight (see Methods for details).

The Cu-IT shows excellent antiviral activity against TMV. Figure 4b shows a photograph of the inoculated (with an initial TMV concentration of 500 ng ml^{-1}, a highly infectious dose) *N. tabaccum* leaves (after 5 days); the leaf on the left was inoculated with TMV being treated using Cu-IT or unmodified textile for 3 h, and the one on the right with TMV being treated for 24 h. No lesions are observed on the halves inoculated with Cu-IT-treated TMV and a 3 h treatment is sufficient for the Cu-IT to take effect (left leaf in Fig. 3b), while a large number of lesions are observed on the halves inoculated with the unmodified textile-treated TMV and the lesion count is higher for TMV treated for 24 h. A quantitative analysis of the lesion count variation versus the initial TMV solution concentration and of the time for unmodified textile or Cu-IT treatment (3 and 24 h) is shown in Fig. 3c. The *N. tabaccum* leaves inoculated with Cu-IT-treated TMV yield zero counts under all conditions. These results strongly indicate that the TMV infectivity can be effectively inhibited after exposure to the Cu-IT for a period as short as 3 h. Considering that TMV shows very high stability under various conditions[40,41], the Cu-IT demonstrates strong potential for use as an antiviral material with high efficacy against a broader range of virus strains[42–45].

We also evaluated the inhibitory effect of Cu-IT on IAV using a plaque assay (Fig. 3d). When the Cu-IT was incubated with a low concentration of IAV solution (~3×10^4 p.f.u. ml^{-1}), the infectivity reduced significantly, 567-fold lower than the IAV solution incubated with no textile. In contrast, IAV incubated with the unmodified textile also resulted in a decrease in infectivity, but far less (4-fold). Moreover, when the Cu-IT was incubated with a high concentration of the IAV solution (~3×10^6 p.f.u. ml^{-1}), no plaque was found, while a low decrease of infectivity (22.5-fold) was measured for the unmodified textile. We noted that the result of 60 p.f.u. ml^{-1} in the case of a low concentration of IAV solution incubated with Cu-IT was caused by either cross-contamination or was a stochastic effect due to very low virus titre, as we retested the Cu-IT with and without wash by focus assay and did not find any foci (Supplementary Table 3). These results demonstrate the Cu-IT's superior inhibitory activity against IAV.

The colony numbers for the Cu-IT-treated bacterial cultures (for all four strains: the Gram-negative bacteria *E. coli*, *S. typhimurium* and *P. aeruginosa*, and the Gram-positive bacterium *B. subtilis*) were significantly lower than those for the unmodified textile-treated cultures (Fig. 3e). We quantified these results using colony-forming units (c.f.u.)

Fig. 4 | The mechanical properties and stability of the Cu-IT. a, Photographs showing the Cu-IT maintaining its shape after crumpling and unfolding. **b**, Photographs of a Cu-IT being washed based on the international standard ISO 6330-2012. **c**,**d**, The Cu K-edge XANES (**c**) and *k*-space EXAFS (**d**) spectra of the washed Cu-IT sample. **e**, X-ray diffraction patterns of the Cu-IT samples after different washing cycles. The Cu-IT samples were prepared after 1, 5, 10 and 50 washing cycles, and the washing time for every cycle was 15 min. **f**, Average half-leaf lesion counts of the leaves that had been inoculated with different TMV solutions. TMV solutions with an initial concentration of 500 mg ml^{-1} were pretreated with the washed Cu-IT for 3 h. The error bars represent the standard deviation of half-leaf lesion count. **g**, c.f.u. counts measured from the LB agar plates after the inoculation and overnight incubation of the washed Cu-IT samples treated with cultures of *E. coli*, *S. typhimurium*, *P. aeruginosa* and *B. subtilis* bacteria. The Cu-IT samples were prepared after different washing cycles and the c.f.u. counts are normalized to that of the unwashed Cu-IT sample. The error bars represent the standard deviation of normalized c.f.u. count. **h**, The tensile strength of unmodified cotton textile, textile treated with 10% NaOH (Textile-NaOH) and Cu-IT. The error bars represent the standard deviation of tensile strength.

counts (Fig. 3f) and found the viable cell count in the Cu-IT-treated cultures of *E. coli*, *S. typhimurium*, *P. aeruginosa* and *B. subtilis* were 1,000,000-fold, 8-fold, 10,000,000-fold and 40,000-fold lower than those in the unmodified textile-treated cultures. Note that varied bacteriostatic activities were observed for the four bacterial strains, which may be due to the differences in their cell membrane structures as well as their response to copper-induced ROS[27]. However, detailed mechanistic studies are outside the scope of the current contribution. We further compared the antiviral and antibacterial performance of the Cu-IT with that of various commercial antimicrobial materials and confirmed Cu-IT efficacy (Supplementary Fig. 10).

To study the biocompatibility of the Cu-IT with human skin, we performed a cytotoxicity assessment using artificial perspiration on human dermal fibroblasts. The results demonstrate that the Cu-IT does

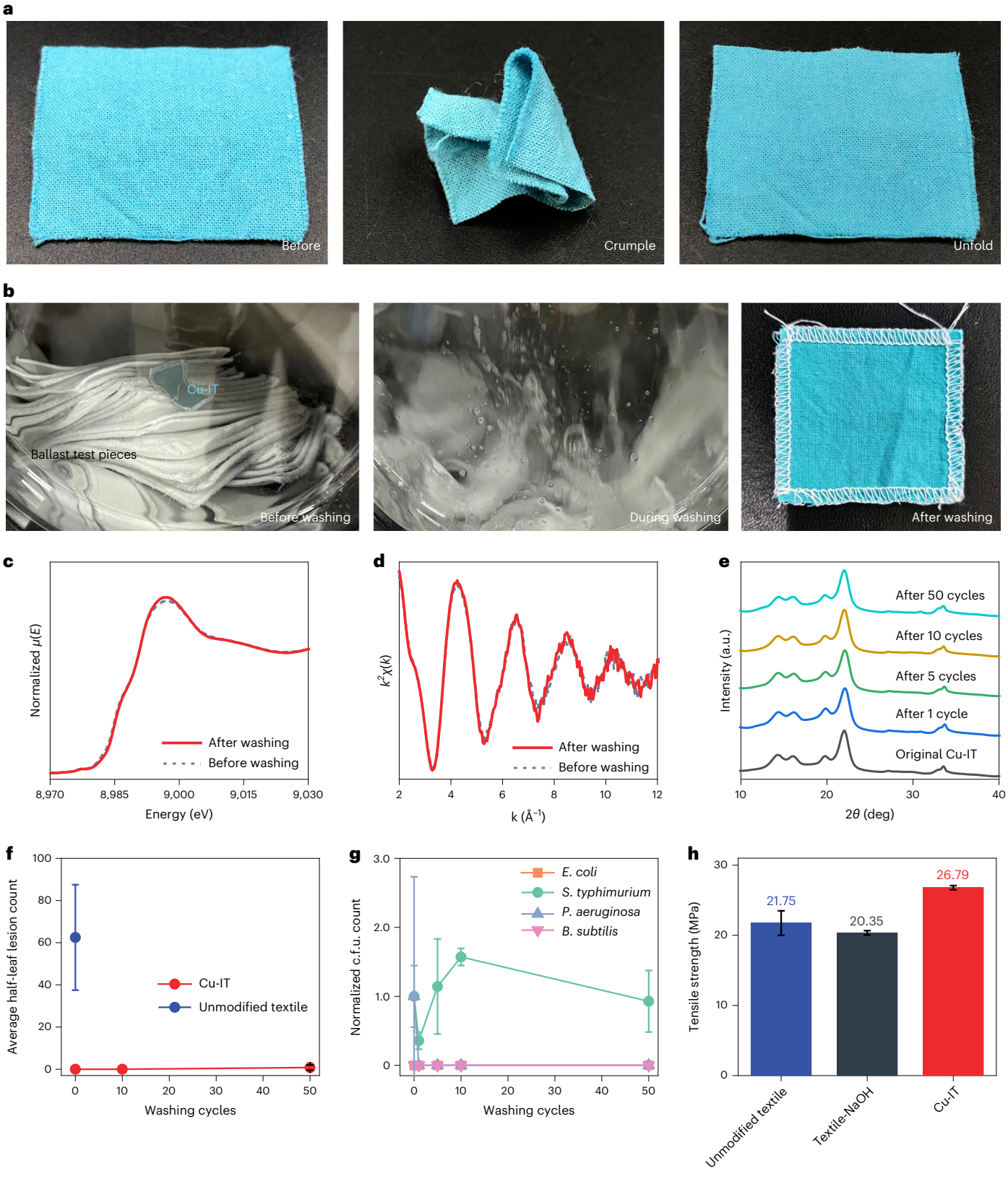

https://doi.org/10.1038/s41565-022-01278-y

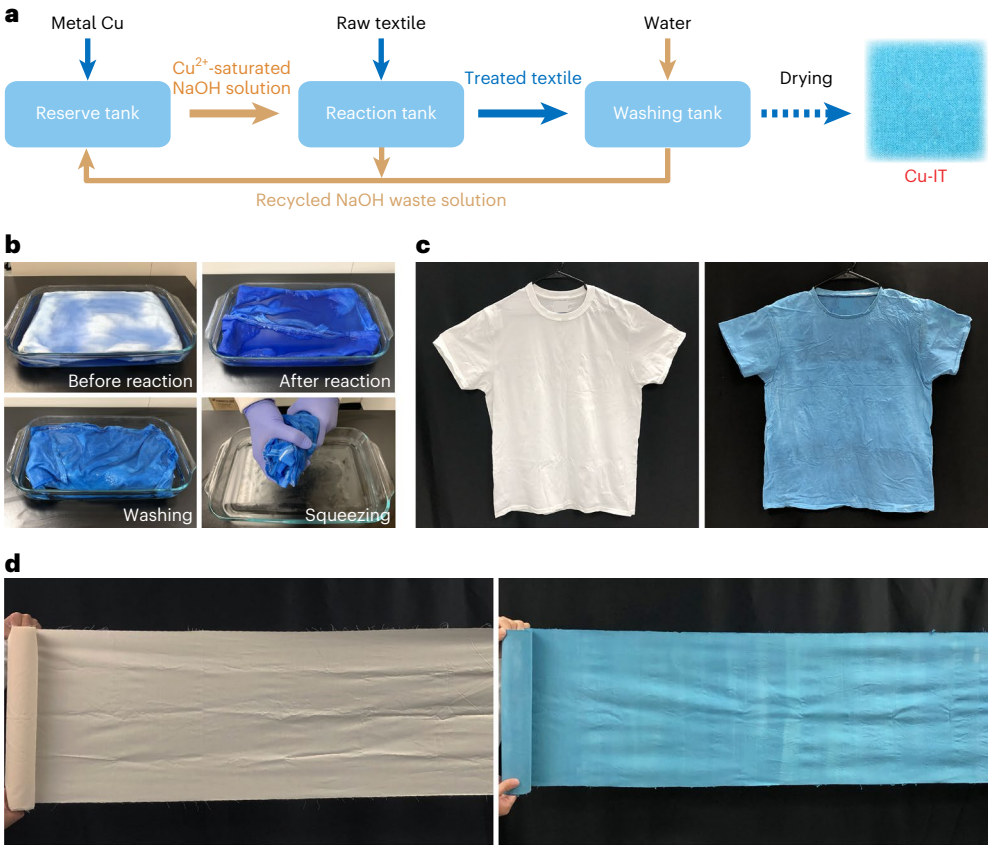

Fig. 5 | Scalable production of the Cu-IT. a, The fabrication process of the Cu-IT using recycled NaOH solution. **b**, Photographs showing the fabrication process of a Cu-IT T-shirt. **c**, Photographs of the pristine cotton T-shirt (left) and the Cu-IT T-shirt (right). **d**, Photographs of the pristine unbleached cotton cloth (left) and the Cu-IT cloth (right).

not cause cytotoxicity due to ions produced from the contact between Cu-IT and human perspiration (Supplementary Fig. 11). In summary, the observed antiviral and bacteriostatic properties suggest that the Cu-IT has high application potential in personal, clinical and medical environments, although follow-on toxicity analysis utilizing mammalian cells and tissues will ensure safe implementation.

Mechanical properties and stability

We also assessed the mechanical properties and washing stability of the Cu-IT. The textile could be folded, crumpled and unfolded without issue, showing general characteristics comparable to those of unmodified textiles (Fig. 4a), which we attribute to the well-preserved structures of the cellulose microfibres and macroscopic material integrity during treatment by the Cu(II)-saturated NaOH solution (Fig. 2d–g and Supplementary Fig. 5).

To test the material's washing stability in water with detergent, a piece of Cu-IT was washed and dried according to the international standard ISO 6330-2012 (Fig. 4b), with no apparent changes of colour or decreased integrity observed. We further verified that the coordinated structures were maintained using XAS (Fig. 4c,d and Supplementary Table 2) and X-ray diffraction (Fig. 4e). The Cu K-edge XANES and EXAFS spectra of the Cu-IT before and after washing were almost identical (the lines are essentially superimposed), and the X-ray diffraction profiles show nearly the same diffraction patterns. Furthermore, we measured the copper concentration in the wash wastewater from a modified (non-ISO) wash test (Supplementary Note 4) and, using a relationship between leached copper over time, estimated that the Cu-IT should endure thousands of washing cycles before reaching its copper half-life time (when the copper content in the Cu-IT decreases to half of its original value; Supplementary Figs. 12 and 13, and Supplementary Note 4). This is longer than the typical lifespan of 200 wash–use cycles for cotton fabric. We also further assessed the antiviral and antibacterial performance of the washed Cu-IT samples and found the antiviral (Fig. 4f and Supplementary Fig. 14) and antibacterial (Fig. 4g) activities generally did not decay after repeated washing, suggesting textile reusability. The data for *S. typhimurium* seemed to indicate that after the first wash, the potency was reduced. This suggests there may be bacterial strain selectivity in antibacterial efficacy, but this would certainly be understandable and would warrant additional study prior to commercialized use.

No structural change was observed in the X-ray diffraction profiles of the Cu-IT stored for over 1 yr under ambient conditions (Supplementary Fig. 15). Additionally, we confirmed the good stability of Cu-IT against ultraviolet, heat and sweat (Supplementary Figs. 16 and 17). To investigate the durability of Cu-IT against abrasion during normal wear use, we performed abrasion-resistance tests on the Cu-IT and unmodified textile (Supplementary Fig. 18). After the abrasion tests, no apparent decrease of integrity was observed in the Cu-IT, while a rupture of the fibres occurred for the unmodified textile. Additionally, the Cu-IT maintained its copper content after abrasion, indicative of the even distribution of copper ions throughout the fibres, which should ensure excellent antiviral and antibacterial performance during everyday use.

Uniaxial tensile tests were performed to quantify the mechanical performance (Fig. 4h). The tensile strength of Cu-IT was 26.79 MPa, which is ~23% higher than that of the unmodified textile (21.75 MPa). In addition, cotton textile treated solely with aqueous NaOH solution, a process also known as mercerization, showed the lowest strength of 20.35 MPa (Supplementary Fig. 19), which may be attributed to the decrease of the degree of polymerization of the cellulose polymers caused by the concentrated NaOH[46,47]. Interestingly, the fracture

properties of the Cu-IT are different to those of the unmodified textile. The fracture area of the Cu-IT is compact with a granular-type fracture, while that of the unmodified textile is loose with a fibrillary-type fracture (Supplementary Fig. 20)[48,49]. These observations demonstrate that the copper coordination within the microfibres improves the mechanical properties of the Cu-IT and highlights the critical role of copper ions in stabilizing the secondary structure of cellulose.

Demonstration of scalable production

We suggest the three-step process (Fig. 5a) for fabricating the Cu-IT is scalable using a roll-to-roll production method, such as that outlined in Supplementary Fig. 21, which comprises the preparation of Cu(II)-saturated NaOH solution, coordination between Cu(II) ions and cellulose molecules via simple soaking, and finally, washing and drying. In addition, NaOH solution can be recycled, and metal copper is the only consumed raw material, making the process cost-effective and sustainable. Figure 5b shows an example of the fabrication scale-up, where a Cu-IT T-shirt was produced from a commercially available cotton T-shirt. The original cotton T-shirt was placed in a 300 mm × 200 mm × 30 mm container filled with Cu(II)-saturated NaOH solution (Supplementary Fig. 22) and soaked for ~7 days until the colour turned blue. After washing and drying, the resultant Cu-IT T-shirt (Fig. 5c) exhibited well-preserved physical properties but slight shrinkage, which may be due to the alkaline solution treatment and the copper-ion coordination. As another example, a roll of Cu-IT cloth 35 cm wide and 280 cm long was prepared from unbleached cotton cloth using the same method (Fig. 5d). It is worth also noting the inherent colour of the Cu-IT is similar to personal protective equipment (PPE) that is commonly used in healthcare settings. Thus, it renders another advantage of mitigating the environmental impact associated with the dyeing process[50,51]. Altogether, this highly scalable, low-cost and ecofriendly fabrication process endows the Cu-IT with great potential for practical use.

Conclusions

We have demonstrated a simple, cost-effective method for efficiently fabricating antiviral and antibacterial textiles by incorporating copper ions into cotton textiles at the molecular level. We showed that copper ions diffuse into the cotton textiles under alkaline conditions and coordinate with oxygen atoms of the hydroxyl groups on cellulose molecules and remain stabilized in the cellulose matrix after washing the textile to a neutral state. The Cu-IT shows high antiviral activity against the TMV and IAV and antibacterial activity against *E. coli*, *S. typhimurium*, *P. aeruginosa* and *B. subtilis* due to the sterilization and disinfection efficacy of copper. The Cu-IT material is also stable and reusable and can sustain repeated washing and wearing. In addition, the coordination bonding enhances the mechanical strength of the modified cotton textile. This fabrication method is highly scalable and shows great potential for mass production of antiviral and antibacterial textiles used in household products, public facilities and medical settings.

Online content

Any methods, additional references, Nature Portfolio reporting summaries, source data, extended data, supplementary information, acknowledgements, peer review information; details of author contributions and competing interests; and statements of data and code availability are available at https://doi.org/10.1038/s41565-022-01278-y.

References

1. Kozel, T. R. & Burnham-Marusich, A. R. Point-of-care testing for infectious diseases: past, present, and future. *J. Clin. Microbiol.* **55**, 2313–2320 (2017).
2. Sohrabi, C. et al. World Health Organization declares global emergency: a review of the 2019 novel coronavirus (COVID-19). *Int. J. Surg.* **76**, 71–76 (2020).
3. Amanat, F. & Krammer, F. SARS-CoV-2 vaccines: status report. *Immunity* **52**, 583–589 (2020).
4. Sidwell, R. W., Dixon, G. J. & Mcneil, E. Quantitative studies on fabrics as disseminators of viruses: I. Persistence of vaccinia virus on cotton and wool fabrics. *Appl. Environ. Microbiol.* **14**, 55–59 (1966).
5. Dixon, G. J., Sidwell, R. W. & Mcneil, E. Quantitative studies on fabrics as disseminators of viruses: II. Persistence of poliomyelitis virus on cotton and wool fabrics. *Appl. Environ. Microbiol.* **14**, 183–188 (1966).
6. Sidwell, R. W., Dixon, G. J., Westbrook, L. & Forziati, F. H. Quantitative studies on fabrics as disseminators of viruses: IV. Virus transmission by dry contact of fabrics. *Appl. Environ. Microbiol.* **19**, 950–954 (1970).
7. Gerba, C. P. & Kennedy, D. Enteric virus survival during household laundering and impact of disinfection with sodium hypochlorite. *Appl. Environ. Microbiol.* **73**, 4425–4428 (2007).
8. Katoh, I. et al. Potential risk of virus carryover by fabrics of personal protective gowns. *Front. Public Health* **7**, 121 (2019).
9. Ansell, M. P. & Mwaikambo, L. Y. in *Handbook of Textile Fibre Structure* Vol. 2 (eds Eichhorn, S. J. et al.) 62–94 (Woodhead, 2009).
10. Hu, L. et al. Stretchable, porous, and conductive energy textiles. *Nano Lett.* **10**, 708–714 (2010).
11. Lei, L., Li, S. & Gu, Y. Cellulose synthase complexes: composition and regulation. *Front. Plant Sci.* **3**, 75 (2012).
12. Turner, S. & Kumar, M. Cellulose synthase complex organization and cellulose microfibril structure. *Philos. Trans. A Math. Phys. Eng. Sci.* **376**, 20170048 (2018).
13. Vasilev, K. Nanoengineered antibacterial coatings and materials: a perspective. *Coatings* **9**, 654 (2019).
14. Zhou, J., Hu, Z., Zabihi, F., Chen, Z. & Zhu, M. Progress and perspective of antiviral protective material. *Adv. Fiber Mater.* **2**, 123–139 (2020).
15. Cloutier, M., Mantovani, D. & Rosei, F. Antibacterial coatings: challenges, perspectives, and opportunities. *Trends Biotechnol.* **33**, 637–652 (2015).
16. Karim, N. et al. Sustainable personal protective clothing for healthcare applications: a review. *ACS Nano* **14**, 12313–12340 (2020).
17. Balasubramaniam, B. et al. Antibacterial and antiviral functional materials: chemistry and biological activity toward tackling COVID-19-like pandemics. *ACS Pharmacol. Transl. Sci.* **4**, 8–54 (2021).
18. Hassabo, A. G., El-Naggar, M. E., Mohamed, A. L. & Hebeish, A. A. Development of multifunctional modified cotton fabric with tri-component nanoparticles of silver, copper and zinc oxide. *Carbohydr. Polym.* **210**, 144–156 (2019).
19. Suryaprabha, T. & Sethuraman, M. G. Fabrication of copper-based superhydrophobic self-cleaning antibacterial coating over cotton fabric. *Cellulose* **24**, 395–407 (2016).
20. Xu, Q. et al. Preparation of copper nanoparticles coated cotton fabrics with durable antibacterial properties. *Fibers Polym.* **19**, 1004–1013 (2018).
21. Ali, A. et al. Copper coated multifunctional cotton fabrics. *J. Ind. Text.* **48**, 448–464 (2017).
22. Anita, S., Ramachandran, T., Rajendran, R., Koushik, C. V. & Mahalakshmi, M. A study of the antimicrobial property of encapsulated copper oxide nanoparticles on cotton fabric. *Text. Res. J.* **81**, 1081–1088 (2011).
23. Galdiero, S. et al. Silver nanoparticles as potential antiviral agents. *Molecules* **16**, 8894–8918 (2011).
24. Monette, A. & Mouland, A. J. Zinc and copper ions differentially regulate prion-like phase separation dynamics of pan-virus nucleocapsid biomolecular condensates. *Viruses* **12**, 1179 (2020).

25. Tavakoli, A. & Hashemzadeh, M. S. Inhibition of herpes simplex virus type 1 by copper oxide nanoparticles. *J. Virological Methods* **275**, 113688 (2020).
26. Fang, L. et al. Impact of cell wall structure on the behavior of bacterial cells in the binding of copper and cadmium. *Colloids Surf. A Physicochem. Eng. Asp.* **347**, 50–55 (2009).
27. Grass, G., Rensing, C. & Solioz, M. Metallic copper as an antimicrobial surface. *Appl. Environ. Microbiol.* **77**, 1541–1547 (2011).
28. Warnes, S. L., Caves, V. & Keevil, C. W. Mechanism of copper surface toxicity in *Escherichia coli* O157:H7 and *Salmonella* involves immediate membrane depolarization followed by slower rate of DNA destruction which differs from that observed for Gram-positive bacteria. *Environ. Microbiol.* **14**, 1730–1743 (2012).
29. Lemire, J. A., Harrison, J. J. & Turner, R. J. Antimicrobial activity of metals: mechanisms, molecular targets and applications. *Nat. Rev. Microbiol.* **11**, 371–384 (2013).
30. Isogai, A. NMR analysis of cellulose dissolved in aqueous NaOH solutions. *Cellulose* **4**, 99–107 (1997).
31. Philipp, B., Kunze, J. & Fink, H. P. in *The Structures of Cellulose* Vol. 340 (ed. Atalla, R. H.) Ch. 1 (American Chemical Society, 1987).
32. Gaspar, D. et al. Nanocrystalline cellulose applied simultaneously as the gate dielectric and the substrate in flexible field effect transistors. *Nanotechnology* **25**, 094008 (2014).
33. Li, T. et al. Cellulose ionic conductors with high differential thermal voltage for low-grade heat harvesting. *Nat. Mater.* **18**, 608–613 (2019).
34. Ogawa, Y. et al. Formation and stability of cellulose–copper–NaOH crystalline complex. *Cellulose* **21**, 999–1006 (2013).
35. Yang, C. et al. Copper-coordinated cellulose ion conductors for solid-state batteries. *Nature* **598**, 590–596 (2021).
36. Rupp, H. & Weser, U. X-ray photoelectron spectroscopy of copper(II), copper(I), and mixed valence systems. *Bioinorg. Chem.* **6**, 45–59 (1976).
37. Biesinger, M. C. Advanced analysis of copper X-ray photoelectron spectra. *Surf. Interface Anal.* **49**, 1325–1334 (2017).
38. Lu, Q., Gao, F. & Komarneni, S. Cellulose-directed growth of selenium nanobelts in solution. *Chem. Mater.* **18**, 159–163 (2006).
39. Zhang, D. Y. et al. Microwave-assisted synthesis of PdNPs by cellulose solution to prepare 3D porous microspheres applied on dyes discoloration. *Carbohydr. Polym.* **247**, 116569 (2020).
40. Creager, A. N. *The Life of a Virus: Tobacco Mosaic Virus as an Experimental Model, 1930–1965* (University of Chicago Press, 2002).
41. Scholthof, K. B. Tobacco mosaic virus: a model system for plant biology. *Annu. Rev. Phytopathol.* **42**, 13–34 (2004).
42. Caspar, D. L. D. in *Advances in Protein Chemistry* Vol. 18 (eds Anfinsen, C. B. et al.) 37–121 (Academic Press, 1964).
43. Noyce, J. O., Michels, H. & Keevil, C. W. Inactivation of influenza A virus on copper versus stainless steel surfaces. *Appl. Environ. Microbiol.* **73**, 2748–2750 (2007).
44. Borkow, G., Lara, H. H., Covington, C. Y., Nyamathi, A. & Gabbay, J. Deactivation of human immunodeficiency virus type 1 in medium by copper oxide-containing filters. *Antimicrob. Agents Chemother.* **52**, 518–525 (2008).
45. Warnes, S. L. & Keevil, C. W. Inactivation of norovirus on dry copper alloy surfaces. *PLoS ONE* **8**, e75017 (2013).
46. Knill, C. J. & Kennedy, J. F. Degradation of cellulose under alkaline conditions. *Carbohydr. Polym.* **51**, 281–300 (2003).
47. Shao, C. et al. Mechanism for the depolymerization of cellulose under alkaline conditions. *J. Mol. Modeling* **24**, 124 (2018).
48. Hearle, J. W. S. & Sparrow, J. T. Further studies of the fractography of cotton fibers. *Text. Res. J.* **49**, 268–282 (1979).
49. Hearle, J. W. S. in *Fiber Fracture* (eds Elices, M. & Llorca, J.) 57–71 (Elsevier, 2002).
50. Mia, R. et al. Review on various types of pollution problem in textile dyeing & printing industries of Bangladesh and recommandation for mitigation. *J. Tex. Eng. Fash. Technol.* **5**, 220–226 (2019).
51. Lellis, B., Fávaro-Polonio, C. Z., Pamphile, J. A. & Polonio, J. C. Effects of textile dyes on health and the environment and bioremediation potential of living organisms. *Biotechnol. Res. Innov.* **3**, 275–290 (2019).

Methods

Preparation of the Cu-IT

NaOH solutions of 5, 10, 20, and 40 wt% were prepared by dissolving NaOH (Sigma-Aldrich) in DI water. Cu(II)-saturated NaOH aqueous solution was prepared by immersing copper wires (Alpha Wire Company) in the NaOH solutions, keeping the preparation static until no further darkening of the blue colour was observed (typically in less than 2 days). After that, the cotton textiles were soaked in the Cu(II)-saturated NaOH solutions until they turned into stable blue colour (typically in 3 days). The Cu-IT samples were then washed with DI water several times until the pH value of the waste reached 7, and were then dried at room temperature.

Material characterization

X-ray diffraction measurements. X-ray diffraction experiments were conducted on a Xenocs Xeuss SAXS/WAXS system with a Cu Kα (λ = 1.5418 Å) microfocusing source and a Detris Pilatus 300k detector in transmission mode. The sample-to-detector distance was 135 mm. The textile specimens were mounted in a vacuum chamber to minimize the air background scattering.

TGA. The copper contents of the textiles were determined using a thermogravimetric/differential thermal analysis system (SDT 650, TA instruments) at a heating rate of 5 °C min^{-1} in air.

Mechanical tensile test. The tensile properties of the samples were characterized using an Instron tester with a 1,000 N load cell. The textile samples were 10 mm wide and 50 mm long, and were uniaxially stretched at a strain rate of 0.5 mm min^{-1}. At least five specimens were measured from each type of sample.

Inductively coupled plasma optical emission spectroscopy. The copper concentration in the washing wastewater without dilution was measured by inductively coupled plasma optical emission spectroscopy (Agilent 725ES).

SEM. The morphologies of the textiles were studied by using a scanning electron microscope (Tescan GAIA FEG SEM). The accelerating voltages were 5 or 10 kV. An X-ray detector (AMETEK Octane Plus) was used to perform the EDS.

XPS measurements. XPS was performed on a Kratos Axis 165 X-ray photoelectron spectrometer and the data were analysed by CasaXPS software.

XAS. Cu K-edge XAS was conducted at the Brookhaven National Laboratory (BNL) National Synchrotron Light Source II (NSLS-II) 8-ID ISS beam line[52]. The textile samples were scanned in fluorescence mode at the Cu K-edge over an energy range from 8,700 to 10,000 eV. Two ion chambers with a copper foil in between were positioned behind the sample, which enabled simultaneous measurement of the energy reference. For the EXAFS fitting, data were analysed using WinXAS 3.1 software[53]. EXAFS fits were obtained using a least-squares fit in *r* space of the isolated Fourier transform of the k^2-weighted data. A Cu–O scattering path was created using a dehydrated C (II) acetate reference, which has four Cu–O bonds. The copper textile samples were fitted using that scattering path. A standard procedure was employed to obtain coordination numbers and bond distances.

Washing test

The washing and drying procedures used to test the Cu-IT were based on an international standard (ISO 6330-2012). A front-loading, horizontal-drum-type washing machine (FOM71 CLS) was used. A piece of Cu-IT sample (5 cm × 5 cm) was loaded into the washing machine with sufficient ballast test pieces (100% knitted polyester texturized filament fabric) and 20 g of non-phosphate detergent (ECE reference detergent 98). The 4M washing procedure was applied, in which the wash time was 15 min and the wash temperature was 40 °C. Three rinse steps were applied after washing, with rinse times of 3, 2 and 2 min, respectively. After rinsing, the Cu-IT sample was removed from the machine and, without extracting the water, suspended from a line in still air at room temperature and allowed to dry. For the modified washing tests, the Cu-IT samples were extensively washed in a vigorously stirred (1,000 r.p.m.) water bath with detergent added. Specifically, a piece of Cu-IT 9 cm × 4.5 cm in size was immersed into ~200 ml of water with 1 g of detergent.

Abrasion resistance test

The abrasion resistance tests on the unmodified textile and Cu-IT samples were performed according to an international standard (ISO12947-2:2016). Textile samples with a diameter of 38 mm and wool abradant fabrics with a diameter of 120 mm were mounted on a Martindale machine (YG401F, Wenzhou Fangyuan Instrument). The effective mass of the abrasion load was 2.5 kg. The textile samples were abraded for 10,000 rubs with an inspection interval after every 2,000 rubs.

Ultraviolet stability test

The Cu-IT samples were placed under an ultraviolet lamp (emission wavelength, 405 nm; output power, 60 W; Geeetech) for different times.

Thermal stability test

The Cu-IT samples were placed in an oven (Across International) at 75 °C for different times.

Sweat stability test

The Cu-IT samples were soaked in artificial human sweat for different times. That is, a human sweat mimic was prepared based on an international standard (ISO 105-E04:1989(E)). Specifically, 0.5 g of L-histidine monohydrochloride monohydrate, 5 g of NaCl and 2.5 g of $Na_2HPO_4{\cdot}2H_2O$ were dissolved in 1 litre of water and then brought to pH 8 with 0.1 mol l^{-1} NaOH solution.

Antiviral and antibacterial assessment

For both antiviral and antibacterial assessment assays, textile samples 16 mm in diameter were used. Prior to each assay, the textile samples were sterilized by sonicating in 98% isopropanol for 5 min and were washed twice with sterile water.

To assess the antiviral capabilities against TMV, the textile samples were incubated in TMV solutions in pH 7.4 phosphate-buffered saline (PBS), ranging from 0 to 500 ng ml^{-1}. Samples of TMV solution were taken at 3 and 24 h of incubation and were kept at −20 °C. Half-leaf assays were done as previously described[54]. Specifically, leaves of ~6- to 8-week-old *N. tabaccum* cv. Xanthi nc plants were dusted with carborundum, and half of each leaf was inoculated with 20 µl of a TMV solution sample that had been incubated in the presence of Cu-IT, while the other half of the leaf was inoculated with a TMV control solution of the same concentration that had been incubated with the unmodified textile. Plants were grown for an additional 5 days and local lesions corresponding to TMV infection foci were counted.

To assess the antiviral capabilities against IAV, the Puerto Rico/8/34 IAV strain was propagated in MDCK cells. The virus stock was used as a high-concentration virus solution (~3×10^6 p.f.u. ml^{-1}) or diluted in Dulbecco's PBS containing 0.1% bovine serum albumin to a lower concentration (~3×10^4 p.f.u. ml^{-1}). Textile samples were incubated in 500 µl of high- or low-concentration IAV solution at room temperature for 30 min. Virus-containing supernatants were recovered and stored at −80 °C until further analyses. Plaque assays were carried out using MDCK cells, as previously described[55]. Briefly, virus solutions incubated with and without Cu-IT were serially diluted in DMEM

containing 1.5 μg ml^{-1} TPCK-treated trypsin and no serum, and 100 μl of each dilution was inoculated on confluent MDCK cells in 12-well plates. Following a 1 h adsorption at 37 °C, cells were washed twice with Dulbecco's PBS and overlaid with DMEM containing 1% SeaPlaque agarose, 10 mM HEPES buffer, 1.5 μg ml^{-1} TPCK-treated trypsin, 100 U ml^{-1} penicillin and 100 mg ml^{-1} streptomycin. After incubation at 37 °C in 5% CO_2 for 3 days, cells were stained with 0.01% neutral red to allow plaque visualization and counting. The number of p.f.u. per millilitre in the undiluted solutions was calculated by multiplying the number of plaques by the dilution factors.

To assess the antibacterial activity, we tested the textile samples with liquid bacterial cultures. *E. coli* SW101, *S. typhimurium*, *P. aeruginosa* and *B. subtilis* seed cultures were prepared overnight in LB media at 37 °C and 250 r.p.m. shaking. Overnight cultures were then diluted to approximately 0.1 OD_{600} (optical density at 600 nm) in M9 minimal media with 0.4% glucose and 0.4% casamino acids for *E. coli* SW101, *S. typhimurium* and *P. aeruginosa*, and M9 minimal media with 0.4% glucose, 0.4% casamino acids and 0.1% tryptophan for *B. subtilis*. Then, 2 ml of the diluted cultures was plated per well in a 12-well culture plate along with a textile sample. The cultures were then incubated at 37 °C and 250 r.p.m. shaking for 3 h. Bacteria cultures were sampled after 3 h and were serially diluted 10-fold. Then, 5 μl of each serial dilution was plated per dilution in triplicate onto LB agar. After overnight incubation at 37 °C, the plates were imaged and manually counted for colony-forming units.

Cytotoxicity assessment

Primary human dermal fibroblasts (PCS-201-012, ATCC) were cultured in fibroblast basal medium (PCS-201-030, ATCC) supplemented with the Fibroblast Growth Kit, Low Serum (PCS-201-041, ATCC), and 1% (v/v) penicillin/streptomycin (P/S, Gibco), and were incubated in a humidified atmosphere at 37 °C and 5% CO_2. A piece of the textile sample 16 mm in diameter was added to 2 ml of artificial perspiration and incubated at 37 °C for 3 h. At 3 h, the artificial perspiration was collected and filtered through a 0.22 μm syringe filter, then 500 μl was added to a confluent well of primary human dermal fibroblasts, plated in a 24-well plate. The primary human dermal fibroblasts with artificial perspiration were incubated in a humidified atmosphere at 37 °C and 5% CO_2 for 3 h. At 3 h, the artificial perspiration was removed, and cells were stained with a Live/Dead solution of 1 μM calcein AM and 4 μM ethidium homodimer-1. The dead positive control was prepared by incubating cells with ice-cold 70% ethanol for 15 min prior to staining. Each well was stained and protected from light at room temperature for 30 min with 500 μl of textile-treated perspiration. After 30 min, the staining solution was removed, and cells were stored in 500 μl PBS during imaging. Cell counts were quantified from images using ImageJ's particle-counting feature.

Data availability

The data that support the findings of this study are available within the paper and the Supplementary Information. Source data are provided with this paper. Other relevant data are available from the corresponding authors on reasonable request. Source data are provided with this paper.

References

52. Leshchev, D. et al. The Inner Shell Spectroscopy beamline at NSLS-II: a facility for in situ and operando X-ray absorption spectroscopy for materials research. *J. Synchrotron Radiat.* **29**, 1095–1106 (2022).
53. Ressler, T. WinXAS: a program for X-ray absorption spectroscopy data analysis under MS-Windows. *J. Synchrotron Radiat.* **5**, 118–122 (1998).
54. Padmanabhan, M. S., Kramer, S. R., Wang, X. & Culver, J. N. Tobacco mosaic virus replicase-auxin/indole acetic acid protein interactions: reprogramming the auxin response pathway to enhance virus infection. *J. Virol.* **82**, 2477–2485 (2008).
55. Jalily, P. H. et al. Mechanisms of action of novel influenza A/M2 viroporin inhibitors derived from hexamethylene amiloride. *Mol. Pharmacol.* **90**, 80–95 (2016).

Acknowledgements

We acknowledge the support from the University of Maryland A. James Clark School of Engineering. We acknowledge the Maryland Nanocenter, its Surface Analysis Center and the AIM Lab. The XAS measurements in this research used resources at the 8-ID Beamline of the National Synchrotron Light Source II, a US Department of Energy (DOE) Office of Science User Facility operated by Brookhaven National Laboratory under contract number DE-SC0012704, and those of the Advanced Photon Source, a US DOE Office of Science User Facility operated for the DOE Office of Science by Argonne National Laboratory under contract number DE-AC02-06CH11357.

Author contributions

L.H. and J.Q. conceived the idea. J.Q. and D.Z. conducted the material preparation. J.Q. performed the material characterization. J.Q., Q.D. and T.L. analysed the results. X.Z., Y.M. and R.M.B. performed the X-ray diffraction analysis. D.P.D., J.T.M., L.W. and T.W. carried out the XAS measurements and analysis. K.C., J.N.C., S.T., J.R.G., D.K.M. and W.E.B. conducted the antiviral and antibacterial tests. J.Q., Q.D., K.C., D.Z., Y.M. and A.H.B. collectively wrote the paper. L.H. supervised the research. All authors discussed the results and commented on the manuscript.

Competing interests

The authors declare no competing interests.

Additional information

Supplementary information The online version contains supplementary material available at https://doi.org/10.1038/s41565-022-01278-y.

Correspondence and requests for materials should be addressed to William E. Bentley or Liangbing Hu.

Peer review information *Nature Nanotechnology* thanks the anonymous reviewers for their contribution to the peer review of this work.

Disclaimer Certain equipment, instruments, or materials are identified in this paper to adequately specify the experimental details. Such identification does not imply recommendation by the National Institute of Standards and Technology nor does it imply the materials are necessarily the best available for the purpose.